ISSN 1674-1056
http://cpb.iphy.ac.cn
http://iopscience.iop.org/cpb
中国物理 B
Chinese Physics
中国物理
Chinese Physics B

Vibrational effects on electron momentum distributionsof outer valence orbitals of benzene

Yu Zhang(张钰), Shanshan Niu(牛珊珊), Yaguo Tang(唐亚国), Yichun Wang(王忆纯), Xu Shan(单旭), Xiangjun Chen(陈向军)
Citation: Chin. Phys. B . 2020, 29(2): 023402 . **doi:** 10.1088/1674-1056/ab671b
Journal homepage: http://cpb.iphy.ac.cn; http://iopscience.iop.org/cpb

What follows is a list of articles you may be interested in

Differential cross sections for electron impact excitation of molecular hydrogen using the momentum-space multichannel optical method

Yuan-Cheng Wang(王远成), Jia Ma(马佳), Ya-Jun Zhou(周雅君)
Chin. Phys. B . 2016, 25(4): 043401 . **doi:** 10.1088/1674-1056/25/4/043401

Dissociative ionization cross sections of CO_2 at electron impact energy of 5 keV

Wang En-Liang, Shen Zhen-Jie, Yang Hong-Jiang, Tang Ya-Guo, Shan Xu, Chen Xiang-Jun
Chin. Phys. B . 2014, 23(11): 113404 . **doi:** 10.1088/1674-1056/23/11/113404

Electron momentum spectroscopy of NF_3

Li Jia-Ming, Miao Yu-Run, Deng Jing-Kang, Ning Chuan-Gang
Chin. Phys. B . 2014, 23(11): 113403 . **doi:** 10.1088/1674-1056/23/11/113403

Assessment of delocalized and localized molecular orbitals through electron momentum spectroscopy

Liu Yuan, Cheung Ling-Fung, Ning Chuan-Gang
Chin. Phys. B . 2014, 23(6): 063403 . **doi:** 10.1088/1674-1056/23/6/063403

Decay pathways of superexcited states of nitrous oxide

Lin Mei, Liu Ya-Wei, Zhong Zhi-Ping, Zhu Lin-Fan
Chin. Phys. B . 2014, 23(5): 053403 . **doi:** 10.1088/1674-1056/23/5/053403

Vibrational effects on electron momentum distributions of outer valence orbitals of benzene*

Yu Zhang(张钰)†, Shanshan Niu(牛珊珊), Yaguo Tang(唐亚国), Yichun Wang(王忆纯), Xu Shan(单旭), and Xiangjun Chen(陈向军)

Hefei National Laboratory for Physical Sciences at the Microscale and Department of Modern Physics, University of Science and Technology of China, Hefei 230026, *China*

(Received 22 October 2019; accepted manuscript online 3 January 2020)

The outer valence electron momentum distributions of benzene are reinvestigated with theoretical calculations involving the vibrational effects. The results are compared with recent experimental measurements [*Phys. Rev. A* **98** 042705 (2018)]. The significant discrepancies between theories and experiments in previous works have now been interpreted quantitatively, indicating that the vibrational motion in benzene molecule has noticeable influence on its electron momentum distributions.

Keywords: electron momentum spectroscopy, benzene, outer valence orbitals, vibrational effects

PACS: 34.80.Gs, 31.15.aj **DOI:** 10.1088/1674-1056/ab671b

1. Introduction

Since the pioneering works of McCarthy, Weigold, and co-workers[1–3] several decades ago, electron momentum spectroscopy (EMS) has been regarded as one of the robust tools to investigate the electronic structures of atoms and molecules. EMS is based on the high energy electron impact binary (e, 2e) reaction near the Bethe ridge condition.[1–5] Within the framework of plane wave impulse approximation (PWIA) theory,[4] the measured (e, 2e) triple differential cross section (TDCS) is proportional to the modulus square of the electron wave function of the ionized orbital in momentum space, or the electron momentum distribution (EMD), which is kinematically independent. The PWIA is not always valid. An intensity higher than PWIA prediction in low momentum region (usually referred to as turn-up effect) was observed for Xe 4d atomic orbital, which can only be interpreted when considering the distorted wave (DW) effect.[6,7] For some π^* like molecular orbitals,[8,9] the observed turn-up effect was also ascribed to the DW effect based on the fact that the EMD intensity in low momentum region changed with the incident energy.[10,11] But the DW effect is not the only factor leading to this turn-up. For the molecular target, earlier EMS studies[12–15] on H_2 and H_2O showed that the influence of molecular vibration on EMDs was usually negligible. Thus, the equilibrium-geometry-approximation is commonly used in EMS studies. However, recent works have shown that for polyatomic molecules, the vibrational motion can also have noticeable influence on EMDs.[16–24] Watanabe *et al.*[16,17] developed a harmonic analytical quantum mechanical (HAQM) approach to fully estimate vibrational effects on EMDs theoretically. It was demonstrated that not only the low-frequency vibrational modes[21–24] but also the high-frequency ones[19,20] play important roles in interpreting the experimental EMDs. The influence of nuclear dynamics on EMDs can alternatively be analyzed using the Born–Oppenheimer molecular dynamics simulations.[23,25,26]

Benzene, the simplest aromatic hydrocarbon, has a fundamental significance in organic chemistry. As a molecule with high order of D_{6h} symmetry, it is also one of the simplest molecules to contain multi-center π orbitals. A great deal of theoretical works have been carried out on[27–30] benzene to explain the vibrational spectra. Its electronic structures have been extensively studied by photoelectron spectroscopy employing He I, He II radiation[31–33] and x-ray,[34] as well as by theoretical calculations.[35–37] Early EMS studies on the valence shells of benzene were carried out by Fuss *et al.*[38] and Samardzic *et al.*[39] at 1200 eV collision energy. In spite of the poor data statistics, these works did show large discrepancies between experiments and PWIA calculations in the low momentum region for some molecular orbitals (MOs). In order to investigate the reason for the discrepancies, Huang *et al.*[40] conducted a high-resolution EMS study on benzene recently. They examined the influence of the DW effect by performing the experiments at two impact energies of 600 eV and 1200 eV. Part of the discrepancies can be ascribed to the DW effect, while significant disagreement still remains.

In this work, we conduct a comprehensive investigation of vibrational effects on EMDs of benzene using HAQM approach. The result shows that the C–H stretching and C–H bending modes play a crucial role in reproducing the electron momentum profiles of $3e_{2g}$, $1b_{2u}$, and $2b_{1u}$ molecular orbital.

*Project supported by the National Key Research and Development Program of China (Grant No. 2017YFA0402300).

†Corresponding author. E-mail: joeyyu@mail.ustc.edu.cn

© 2020 Chinese Physical Society and IOP Publishing Ltd

2. Theoretical background

EMS is an (e, 2e) experiment in which an incident electron is scattered by a target atom or molecule, and a target electron is ionized simultaneously. Within a series of approximations, including binary encounter and plane wave impulse, the triple differential cross-section for randomly oriented molecules can be expressed as[4]

$$\sigma_{\mathrm{EMS}} = \frac{\mathrm{d}^3\sigma}{\mathrm{d}\Omega_1\,\mathrm{d}\Omega_2\,\mathrm{d}E_1} = (2\pi)^4\,\frac{p_1 p_2}{p_0} f_{\mathrm{ee}} \sum\nolimits_{\mathrm{av}} \langle \boldsymbol{p} f|i\rangle = (2\pi)^4\,\frac{p_1 p_2}{p_0} f_{\mathrm{ee}} M(p), \tag{1}$$

where f_{ee} is the e–e collision factor and $\sum_{\mathrm{av}}$ represents an average over initial $|i\rangle$ and a sum over final $|f\rangle$ degenerate states. $M(p)$ is usually referred to as the structure factor, which is the spherically averaged EMD or electron momentum profile. For a molecular target, the Born–Oppenheimer approximation is commonly applied, in which the total wave function is separated as a product of electronic, vibrational, and rotational wave functions. By ignoring the rotational motions and applying closure relation to the final vibrational eigenstates, the structure factor can be simplified as[4]

$$M(p) = \sum_v p_v(T) \int |\chi_{iv}(\boldsymbol{Q})|^2 \rho_f(p;\boldsymbol{Q})\mathrm{d}\boldsymbol{Q}, \tag{2}$$

where $p_v(T)$ is the Boltzmann's statistical population of the eigenstate v in the ground state at temperature T and $\chi_{iv}(\boldsymbol{Q})$ is the vibrational wave function in the initial state. $\rho_f(p;\boldsymbol{Q})$ is the spherically averaged EMD at a given geometry $\boldsymbol{Q}$, which reads[4]

$$\rho_f(p;\boldsymbol{Q}) = \frac{1}{4\pi} S_f^i \int \left|\phi_f(\boldsymbol{p};\boldsymbol{Q})\right|^2 \mathrm{d}\Omega_p, \tag{3}$$

where the weak-coupling approximation has been used. S_f^i is the pole strength or spectroscopic factor and $\phi_f(\boldsymbol{p};\boldsymbol{Q})$ denotes the momentum space representation of the normalized Dyson orbital.

The vibrational effect can be taking into account using the HAQM approach developed by Watanabe *et al.*[16,17] In this approach, the vibrational wave function is approximated as the product of harmonic oscillator functions $\chi_{iv}(\boldsymbol{Q}) = \prod_L \xi_{v_L}(\boldsymbol{Q}_L)$, where $\boldsymbol{Q}_L$ denotes the displacement from the equilibrium geometry $\boldsymbol{Q}_0$ along the normal coordinate of the L-th vibrational mode. Then the vibrational effects on the electron momentum profiles can be written as a sum of the contribution of each vibrational mode if the cross-terms between the vibrational modes are neglected, which reads[16,17]

$$\begin{aligned} M(p) &= \rho_f(p;\boldsymbol{Q}_0) + \sum_L \Delta M_L(p) \\ &= \rho_f(p;\boldsymbol{Q}_0) + \sum_L \left[\sum_{v_L} p_{v_L}(T) \int |\xi_{v_L}(\boldsymbol{Q}_L)|^2 \right. \\ &\quad \left. \times \rho_f(p;\boldsymbol{Q}_0 + \boldsymbol{Q}_L\hat{q}_L)\,\mathrm{d}\boldsymbol{Q}_L - \rho_f(p;\boldsymbol{Q}_0)\right], \end{aligned} \tag{4}$$

where $\Delta M_L(p)$ is the contribution to the momentum profile through a distortion of the equilibrium geometry along the L-th vibrational mode, and $\hat{\boldsymbol{q}}_L$ is the unit vector along the normal coordinate. The first term is the conventional momentum profile at equilibrium geometry.

Table 1. Vibrational frequencies of benzene: present calculation versus the observation in Ref. [42].

Mode	Main description	Calculated/cm^{-1}	Observed/cm^{-1}
1	C–H out-of-plane bending	1023	993.071
2	C–H stretching in-phase (beat mode)	3193	3073.942
3	C–H in-phase bending	1388	1350
4	C–C–C in-phase puckering (ring deforming)	721	707
5	breathing (ring stretching)	1014	990
6	C–C–C in-phase bending (ring deforming)	623	608.13
7	C–H stretching	3158	3056.7
8	C–C stretching (ring stretching)	1634	1600.9764
9	C–H in-plane bending	1198	1177.776
10	C–H out-of-plane bending (C_6 libration)	871	847.1
11	C–H out-of-plane bending	693	673.97465
12	C–C–C trigonal bending (ring deforming)	1031	1010
13	C–H trigonal stretching	3168	3057
14	C–C stretching (ring stretching)	1334	1309.4
15	C–H in-plane trigonal bending	1173	1149.7
16	C–C–C out-of-plane bending (ring deforming)	412	398
17	C–H out-of-plane bending	996	967
18	C–H in-plane bending	1060	1038.2670
19	C–C stretching (ring stretching)	1516	1483.9854
20	C–H stretching	3183	3064.3674

The Dyson orbital can further be approximated by neutral canonical Hartree–Fock (HF)[2] or Kohn–Sham (KS)[41] orbital. The electron momentum profiles can thus be calculated considering thermally induced nuclear motions using the Boltzmann distribution of vibrational eigenstates at room temperature (298 K). In the present work, the corresponding position-space KS orbital wave functions are calculated by the density functional theory (DFT) method employing Becke three-parameter Lee–Yang–Parr (B3LYP) functional with aug-cc-pVTZ basis sets. The optimized equilibrium geometry, normal coordinates, as well as vibrational frequencies of benzene are also calculated by the same method. There are 30 vibrational modes for benzene molecule, but due to its conspicuous symmetry, 10 vibrational modes are degenerated. The calculated vibrational frequencies are listed in Table 1. As shown in Table 1, the computed frequencies are in good agreement with the observed data.[42] All the calculations are performed using GAUSSIAN 09 program.[43]

For comparison with the experimental data, the finite spectrometer acceptance angles ($\Delta\theta = \pm 0.53^\circ$, $\Delta\phi = \pm 0.84^\circ$) are folded into the calculations.

3. Results and discussion

Benzene molecule contains 12 atoms and 42 electrons. B3LYP/aug-cc-pVTZ theory gives its ground state electronic configuration as

$$(\text{core})^{22}(3a_{1g})^2(2b_{1u})^2(1b_{2u})^2(3e_{1u})^4(1a_{2u})^2(3e_{2g})^4(1e_{1g})^4.$$

Huang *et al.*[40] recently conducted a high-resolution EMS study on benzene to examine the influence of the DW effect on EMDs by performing the experiments at two incident energies of 600 eV and 1200 eV. Part of the discrepancies can be ascribed to the DW effect, while significant disagreement still remains for most of the valence orbitals, especially in the low momentum region. In the present work, theoretical electron momentum profiles (TMPs) for the valence orbitals of benzene are calculated by B3LYP method with aug-cc-pVTZ basis set both at equilibrium geometry (D_{6h} symmetry) and considering the vibrational effects. In order to simplify the discussion, only the experimental electron momentum profiles (XMPs) at higher incident energy of 1200 eV[40] will be invoked for comparison. In Ref. [40], a global normalization factor was determined by fitting the summed experimental distributions of all the valence orbitals to the corresponding PWIA calculations at B3LYP/aug-cc-pVTZ level. The same normalization factor will be used in the present work when comparing with the experiment. The results are shown in Figs. 1–5.

Figure 1 shows the TMPs for the highest occupied molecular orbital $1e_{1g}$ calculated at equilibrium geometry (D_{6h} symmetry) and considering the vibrational effect. The XMP shows a typical p-type character with distinct turn-up in the low momentum region. Huang *et al.* remarked that this turn-up should be ascribed to the DW effect. This can be questioned because there was only unremarkable difference in XMPs when the incident energy changed from 600 eV to 1200 eV. It is worthwhile to explore if the vibrational effect should be responsible for this observed turn-up. However, as can be seen in Fig. 1, the present calculation considering the vibrational effect only predicts a slight non-zero intensity at low momentum, fails to reproduce the significant turn-up at $p < 0.5$ a.u. Other factors such as vibronic coupling need to be explored in the future.

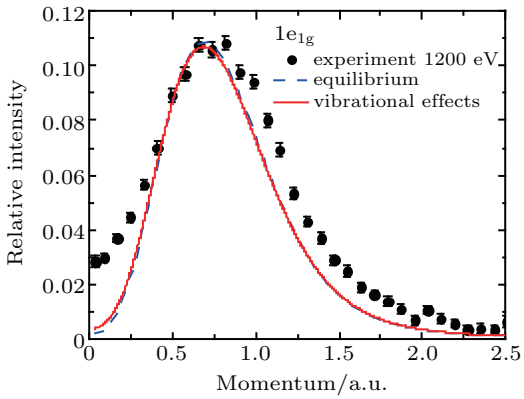


Fig. 1. Theoretical and experimental momentum profiles of $1e_{1g}$ orbital.

The TMP of $3e_{2g}$ orbital based on the equilibrium geometry exhibits a double-hump feature as shown in Fig. 2(a). The calculated result correctly predicts the position of the first hump but significantly underestimates the experimental intensities in the low momentum region. Huang *et al.*[40] demonstrated that high level calculations like B3LYP/aug-cc-pVTZ and symmetry-adapted-cluster configuration-interaction (SAC-CI)/aug-cc-pVTZ do not have notable improvement in reproducing the XMP as compared to the calculation using SCF wavefunction employing (9s5p/4s1p)/[4s2p/2s1p] Gaussian basis set in the early works.[38,39] The experimental intensity of the first hump became lower when the incident energy was changed from 600 eV to 1200 eV,[40] more consistent with the TMPs at equilibrium geometry. This undoubtedly illustrates that the DW effect is surely one of the factors contributing to the turn-up at low momentum in the XMP of this orbital. The large discrepancy between XMP and TMP can further be reduced by including the vibrational effect in the calculation. As shown by the solid red curve in Fig. 2(a), although there is still some discrepancy, the HAQM TMP reproduces the XMP quite well. Contributions from individual vibrational modes (the second term in Eq. (4)) have been analyzed and shown in Fig. 2(b). It can be seen from the figure that the C–H stretching ($\nu 7$) and C–H out-of-plane bending ($\nu 17$) modes dominate the enhancement of the hump at $p \sim 0.5$ a.u., while the C–H trigonal

stretching (ν13) breaks the symmetry and leads to the non-zero intensity at the origin.

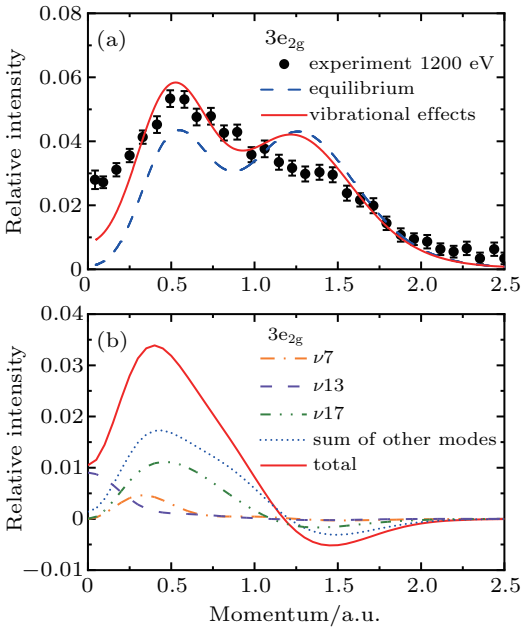


Fig. 2. (a) Theoretical and experimental momentum profiles of $3e_{2g}$ orbital. (b) Contributions from each vibrational mode to the theoretical momentum profile of $3e_{2g}$ orbital.

For the next two orbitals $1a_{2u}$ and $3e_{1u}$, all the TMPs roughly reproduce the shape of the XMPs with some distinct discrepancies in both low and high momentum regions. The TMPs considering the vibrational effect slightly improve the agreement in the maximum regions at $p \sim 0.5$ a.u. for $1a_{2u}$ and at $p \sim 0.3$ a.u. for $3e_{1u}$.

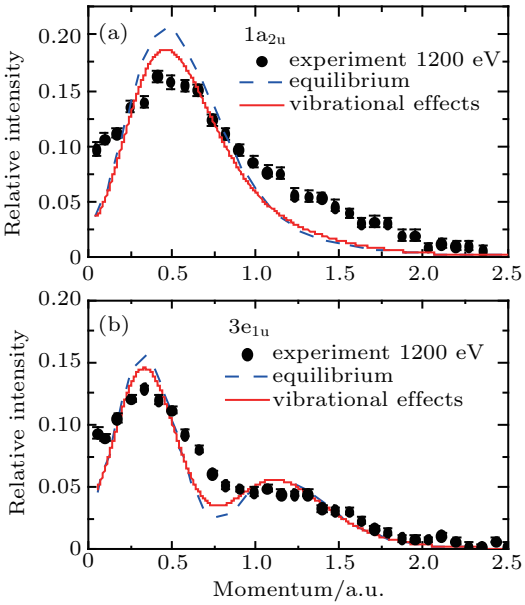


Fig. 3. Theoretical and experimental momentum profiles of (a) $1a_{2u}$ and (b) $3e_{1u}$ orbitals.

Although the energy separations between the ionization peaks of $1b_{2u}$, $2b_{1u}$ and neighboring orbitals are quite small, Huang *et al.*[40] had attempted to resolve the overlapping peaks by Gaussian-function fitting and obtained individual XMPs for $1b_{2u}$ and $2b_{1u}$. The results at 1200 eV incident energy are shown in Figs. 4(a) and 4(b). The TMPs calculated by B3LYP/aug-cc-pVTZ at equilibrium geometry show smooth p-type character with maximum at $p \sim 1.1$ a.u. and $p \sim 0.9$ a.u. for $1b_{2u}$ and $2b_{1u}$, respectively, showing large deviations from the relevant XMPs. Both XMPs have significant non-zero intensity at origin (the turn-up effect). The HAQM TMP for $1b_{2u}$ roughly reproduces both the shape and intensity of the experiment, while the HAQM TMP for $2b_{1u}$ reproduces the shape, especially the distinct turn-up in the low momentum region, but obviously underestimates the intensity in the momentum less than about 1.2 a.u. region. Contributions from individual vibrational modes to the HAQM TMP for these two orbitals have also been analyzed and shown in Figs. 4(c) and 4(d). It can be seen from Fig. 4(c) that the non-zero intensity at $p = 0$ originates from the C–H in-plane trigonal bending mode (ν15). The C–C stretching mode (ν8) dominates the weak hump at $p \sim 0.3$ a.u., while the strong hump at higher momentum can mainly be ascribed to the C–H in-phase stretching (ν2) and C–H in-phase bending (ν3) modes. For $2b_{1u}$, interestingly, the total vibrational effect leads to the intensity enhancement in the low momentum region and attenuation at momentum around 0.8 a.u. The non-zero intensity at $p = 0$ originates from the C–H stretching mode (ν7) and the attenuation at momentum around 0.8 a.u. is mainly contributed by the C–H in-phase stretching (ν2), C–H in-phase bending (ν3) as well as breathing (ring stretching) (ν5) modes. In Ref. [40], Huang *et al.* showed that the intensity of XMP in the low momentum region became lower when the incident energy was increased from 600 eV to 1200 eV,[40] more consistent with the TMPs. This indicates that the DW effect plays an important role in the turn-up effect in XMP of this orbital. The remaining discrepancy between XMP and HAQM TMP at low momentum may be due to that PWIA is still not satisfied even at 1200 eV incident energy. Higher energy experiment or distorted wave calculation[44–46] is expected.

The XMP of the innermost outer valence orbital $3a_{1g}$ exhibits a typical sp-type character as shown in Fig. 5. The TMP calculated at equilibrium geometry shows no distinctive difference from the one calculated considering vibrational motion. This indicates that, for this orbital, the vibrational effect on the electron momentum profile is negligible. By multiplying a factor of 0.8, the TMPs roughly reproduce the XMP both in shape and in intensity. This factor can be regarded as the relative pole strength for this ionization band, in consistent with the pole strength calculated by SAC-CI[40] and ADC(3)[39] methods.

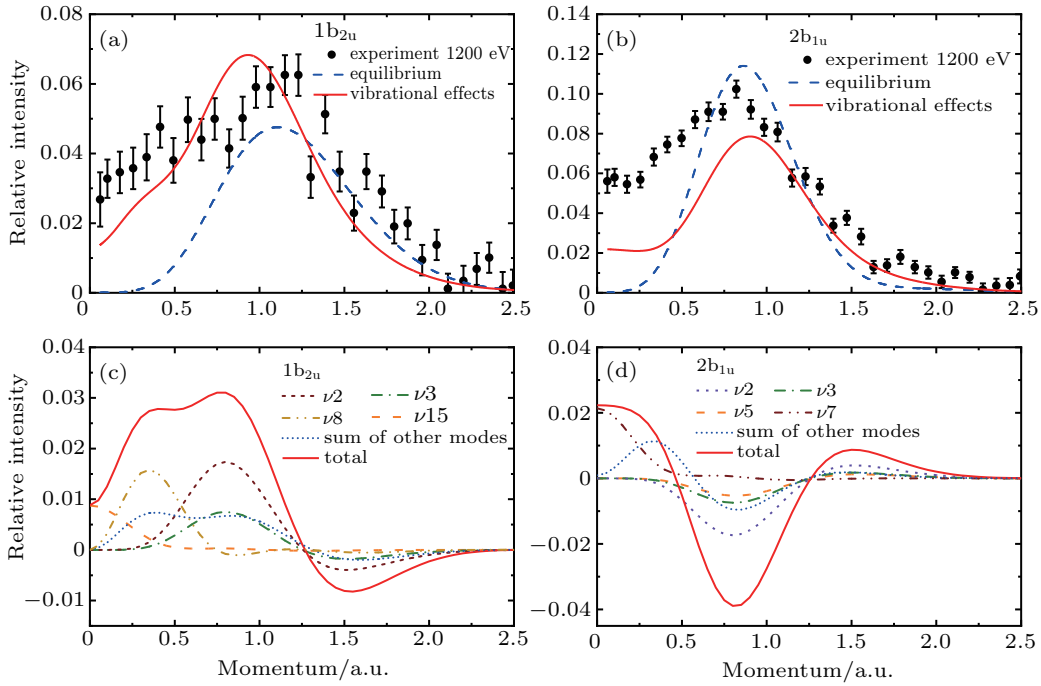


Fig. 4. Theoretical and experimental momentum profiles of (a) $1b_{2u}$, (b) $2b_{1u}$ orbitals and contributions from each vibrational mode to the theoretical momentum profiles of (c) $1b_{2u}$, (d) $2b_{1u}$ orbitals.

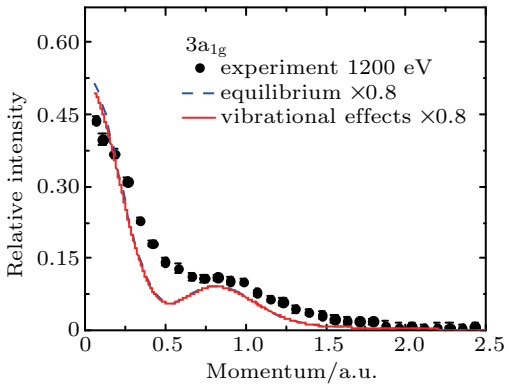


Fig. 5. Theoretical and experimental momentum profiles of $3a_{1g}$ orbital.

4. Summary

The electron momentum distributions for the outer valence orbitals of benzene molecule have been reinvestigated by theoretical calculations considering vibrational motion using harmonic analytical quantum mechanical approach. The results are compared with the calculations at equilibrium geometry and recent experiment[40] at 1200 eV incident electron energy. The significant discrepancies between TMPs calculated at equilibrium geometry and XMPs in previous works have now been interpreted quantitatively, indicating that the vibrational motion in benzene molecule has noticeable influence on its electron momentum distributions. The detailed analysis of the contributions from individual vibrational mode to the TMPs shows that the C–H stretching and C–H bending modes play a crucial role in reproducing the electron momentum profiles of $3e_{2g}$, $1b_{2u}$, and $2b_{1u}$ molecular orbitals.

References

[1] Brion C E 1986 *Int. J. Quantum Chem.* **29** 1397
[2] McCarthy I E and Weigold E 1991 *Rep. Prog. Phys.* **54** 789
[3] Coplan M A, Moore J H and Doering J P 1994 *Rev. Mod. Phys.* **66** 985
[4] Weigold E and McCarthy I E 2012 *Electron Momentum Spectroscopy* (Boston: Springer Science & Business Media)
[5] Takahashi M 2009 *Bull. Chem. Soc. Jpn.* **82** 751
[6] Brunger M J, Braidwood S W, McCarthy I E and Weigold E 1994 *J. Phys. B: At. Mol. Opt. Phys.* **27** L597
[7] Brion C E, Zheng Y, Rolke J, Neville J J, McCarthy I E and Wang J 1998 *J. Phys. B: At. Mol. Opt. Phys.* **31** L223
[8] Ning C G, Ren X G, Deng J K, Su G L, Zhang S F and Li G Q 2006 *Phys. Rev. A* **73** 022704
[9] Ren X G, Ning C G, Deng J K, Zhang S F, Su G L, Huang Y R and Li G Q 2006 *J. Electron. Spectrosc. Relat. Phenom.* **151** 92
[10] Ren X G, Ning C G, Deng J K, Zhang S F, Su G L, Huang F and Li G Q 2005 *Phys. Rev. Lett.* **94** 163201
[11] Wang X, Xu S Y, Ning C G, Al-Hagan O, Hu P F, Zhao Y T, Xu Z F, Deng J K, Wang E L and Ren X G 2018 *Phys. Rev. A* **97** 062704
[12] Dey S, McCarthy I E, Teubner P and Weigold E 1975 *Phys. Rev. Lett.* **34** 782
[13] Bawagan A O, Brion C E, Davidson E R and Feller D 1987 *Chem. Phys.* **113** 19
[14] Leung K T, Sheehy J A and Langhoff P W 1989 *Chem. Phys. Lett.* **157** 135
[15] Lermer N, Todd B R, Cann N M, Zheng Y, Brion C E, Yang Z and Davidson E R 1997 *Phys. Rev. A* **56** 1393
[16] Watanabe N, Yamazaki M and Takahashi M 2012 *J. Chem. Phys.* **137** 114301
[17] Watanabe N, Yamazaki M and Takahashi M 2014 *J. Chem. Phys.* **141** 244314
[18] Morini F, Deleuze M S, Watanabe N and Takahashi M 2015 *J. Chem. Phys.* **142** 094308
[19] Tang Y G, Shan X, Yang J, Niu S S, Zhang Z, Watanabe N, Yamazaki M, Takahashi M and Chen X J 2016 *J. Phys. Chem. A* **120** 6855
[20] Tang Y G, Shan X, Niu S S, Liu Z H, Wang E L, Watanabe N, Yamazaki M, Takahashi M and Chen X J 2017 *J. Phys. Chem. A* **121** 277
[21] Liu K, Ning C G, Luo Z H, Shi L L and Deng J K 2010 *Chem. Phys. Lett.* **497** 229
[22] Miao Y R, Deng J K and Ning C G 2012 *J. Chem. Phys.* **136** 124302
[23] Hajgató B, Morini F and Deleuze M S 2014 *Theoretical Chemistry in Belgium, Highlights in Theoretical Chemistry* Vol. **6** p. 95 (Berlin: Springer)

[24] Yang J, Shan X, Zhang Z, Tang Y G, Zhao M F and Chen X J 2014 *J. Phys. Chem. A* **118** 11780
[25] Hajgató B, Deleuze M S and Morini F 2009 *J. Phys. Chem. A* **113** 7138
[26] Shojaei S R, Vandenbussche J, Deleuze M S and Bultinck P 2013 *J. Phys. Chem. A* **117** 8388
[27] Wilson Jr E B 1934 *Phys. Rev.* **45** 706
[28] Hamdache F, Vergoten G, Lagant P and Benosman A 1989 *J. Raman Spectrosc.* **20** 297
[29] Alcolea Palafox M 2000 *Int. J. Quantum Chem.* **77** 661
[30] Preuss M and Bechstedt F 2006 *Phys. Rev. B* **73** 155413
[31] Åsbrink L, Lindholm E I and Edqvist O 1970 *Chem. Phys. Lett.* **5** 609
[32] Lindholm E and Åsbrink L 1980 *J. Electron. Spectrosc. Relat. Phenom.* **18** 121
[33] Baltzer P, Karlsson L, Wannberg B, Öhrwall G, Holland D, MacDonald M A, Hayes M A and Von Niessen W 1997 *Chem. Phys.* **224** 95
[34] Gelius U, Basilier E, Svensson S, Bergmark T and Siegbahn K 1973 *J. Electron. Spectrosc. Relat. Phenom.* **2** 405
[35] Von Niessen W, Cederbaum L S and Kraemer W P 1976 *J. Chem. Phys.* **65** 1378
[36] Cederbaum L S, Domcke W, Schirmer J, Von Niessen W, Diercksen G and Kraemer W P 1978 *J. Chem. Phys.* **69** 1591
[37] Hirao K and Kato H 1983 *Chem. Phys. Lett.* **98** 340
[38] Fuss I, McCarthy I E, Minchinton A, Weigold E and Larkins F P 1981 *Chem. Phys.* **63** 19
[39] Samardzic O, Brunger M J, Grisogono A M and Weigold E 1993 *J. Phys. B: At. Mol. Opt. Phys.* **26** 3921
[40] Huang Y R, Cai G J and Yu J 2018 *Phys. Rev. A* **98** 042705
[41] Duffy P, Chong D P, Casida M E and Salahub D R 1994 *Phys. Rev. A* **50** 4707
[42] Goodman L, Ozkabak A G and Thakur S N 1991 *J. Phys. Chem.* **95** 9044
[43] Frisch M, Trucks G W, Schlegel H B, Scuseria G E, Robb M A, Cheeseman J R, Scalmani G, Barone V, Mennucci B and Petersson G 2009 *Inc. Wallingford CT* **200** 28
[44] Zhang S B, Li X Y, Wang J G, Qu Y Z and Chen X J 2014 *Phys. Rev. A* **89** 052711
[45] Li X Y, Gong M M, Liu L, Wu Y, Wang J G, Qu Y Z and Chen X J 2017 *Phys. Rev. A* **95** 012703
[46] Li X Y, Ren X G, Hossen K, Wang E L, Chen X J and Dorn A 2018 *Phys. Rev. A* **97** 022706